Journal of Power Sources, 46 (1993) 251–262

A simplified model of the lead/acid battery

Per Ekdunge

Department of Applied Electrochemistry and Corrosion Science, The Royal Institute of Technology, 100 44 Stockholm (Sweden)

Abstract

A mathematical model for the simulation of the lead/acid battery has been developed, based on the physical and chemical processes that occur in the battery. The model is based on theories of porous electrodes and more detailed models of the electrodes and battery that have been published earlier. The model has been simplified by the introduction of integral mean values, thereby reducing the computing time for simulation of the battery. The model can predict limitations of the discharge capacity caused by different phenomena, such as electrolyte depletion in the pores and coverage of the electroactive surface by the precipitated reaction products, as determining by cell geometry and discharged mode. The model shows good agreement with experimental data for discharge, both at constant current and during an electrical-vehicle test cycle.

Introduction

The introduction of new and more advanced applications of batteries has led to an increasing need for simple mathematical models that are able to simulate complicated discharge cycles. Several advanced mathematical models based on the fundamental principles of thermodynamics, reaction kinetics and transport theory have been published, both for the electrodes of the lead/acid battery [1–5] and for the whole cell [6–8]. These mathematical models are valuable tools, in battery research and development, for the analysis and optimization of batteries. For the purpose of the battery user, however, these basic models are often not suitable due to their complexity and the great number of parameters in the models that have to be determined experimentally.

Simple models for the lead/acid battery have also been published. These models are often empirical relations without physical significance. One example that has found application is the Peukert equation [9], which correlates the discharge capacity to the discharge current:

$$t = I^n \tag{1}$$

Kaushik and Mawston [10] proposed a set of equations that predict the battery capacity for a particular rate and temperature. An empirical relation for the change in battery voltage with the depth-of-discharge was developed by Shepherd [11]. This model can only be used to describe discharge with constant current, as is the case with almost all of the simple models. Hyman *et al.* [12] proposed a modification of the Shepherd model to take into account the prehistory of the discharge, which makes the model also usable for discharge with variable rate.

A common model for porous battery electrodes has been proposed by Gidaspow and Baker [13]. This model includes the transformation of one solid into another but

0378-7753/93/$6.00

not the changes in the electrolyte phase. Teutsch *et al.* [14] developed a model for a lead/acid battery with immobilized electrolyte, where the discharge capacity is limited by depletion of sulfuric acid in the porous positive electrode. This model neglects the changes in the solid electrodes.

The aim of the present work was to develop a mathematical model for the lead/acid battery, based on physical and chemical processes in the battery, but sufficiently simplified to make it suitable for battery users in the simulation of different applications. The model should be applicable as a part of a strategy for simulating an entire electrical vehicle without giving rise to prohibitively long computing times.

Model description

The mathematical model for the simulation of the lead/acid battery presented below is based on theories for porous electrodes and more detailed models for the electrodes and battery that have been published earlier [1–8, 15]. The model describes the physical and chemical processes that occur in the different parts of the battery, electrodes and electrolyte, in a simplified way. The main simplification in the model is the introduction of integral mean values that, thereby, avoid integration over the depth of the electrode.

In the model, the electrolyte concentration in the pores of the electrodes, and in the free electrolyte between the electrodes, is calculated by means of a material balance with integral mean values for the concentrations in the different parts of the battery. A unit cell of the battery consists of the electrolyte reservoir between the electrodes and a half lead electrode and a half lead dioxide electrode. This is shown schematically in Fig. 1. The rate of diffusion of sulfuric acid into the electrodes is assumed to be proportional to the concentration difference between the pore electrolyte

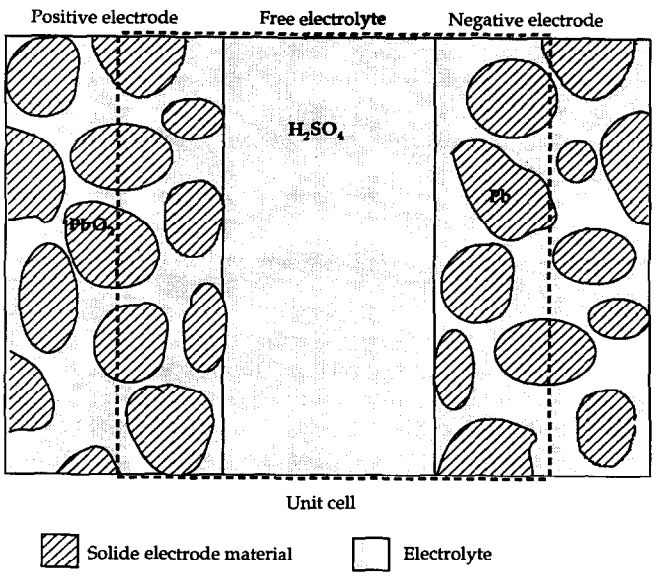

Fig. 1. A one-dimensional macro-homogeneous model for a lead/acid cell.

and the free electrolyte. The equations for the changes in the sulfuric acid concentration in the positive electrode, the negative electrode and the free electrolyte then become:

(i) positive electrode:

$$\bar{C}_{p,t}=\bar{C}_{p,t-1}-\left(\frac{(3-2t_+}{AzF}I-\frac{D_{\text{eff,p}}(\bar{C}_{e,t-1}-\bar{C}_{p,t-1})}{\delta_p}\right)\frac{2\Delta t}{\epsilon_p d_p} \tag{2}$$

(ii) negative electrode:

$$\bar{C}_{n,t}=\bar{C}_{n,t-1}-\left(\frac{(2t_+-1)}{AzF}I-\frac{D_{\text{eff,n}}(\bar{C}_{e,t-1}-\bar{C}_{n,t-1})}{\delta_n}\right)\frac{2\Delta t}{\epsilon_n d_n} \tag{3}$$

(iii) free electrolyte:

$$\bar{C}_{e,t}=\bar{C}_{e,t-1}-\left(\frac{D_{\text{eff,p}}(\bar{C}_{e,t-1}-\bar{C}_{p,t-1})}{\delta_p}+\frac{D_{\text{eff,n}}(\bar{C}_{e,t-1}-\bar{C}_{n,t-1})}{\delta_n}\right)\frac{\Delta t}{d_e} \tag{4}$$

Figure 2 shows how the concentration in the different parts of the lead/acid cell changes with time according to eqns. (2)–(4). The geometric parameters of the cell were taken in accordance with data from Sunu [6] and the value of the diffusion rate (D_{eff}/δ) was fitted to give good agreement with the concentration profiles calculated by Sunu [6] using a complete model.

A voltage balance over the cell gives:

$$E_{\text{cell}}=E_0-IR_e-\eta_+-\eta_- \tag{5}$$

where E_0 is the equilibrium voltage of the cell at time t; R_e is the resistance of the electrolyte between the electrodes; η_+ is the overvoltage at the positive electrode; η_- is the overvoltage at the negative electrode.

The two first term, E_0 and R_e can easily be calculated if the concentration of the sulfuric acid and the geometry of the cell are known. The electrode overvoltages consist of a combination of resistances in the pore electrolyte, the solid electrode materials and the electrochemical reaction. The reaction overvoltages are given by the Butler–Volmer equation which, for higher overvoltages, can be simplified to the Tafel equation, i.e.:

$$\eta=a+b\log i \tag{6}$$

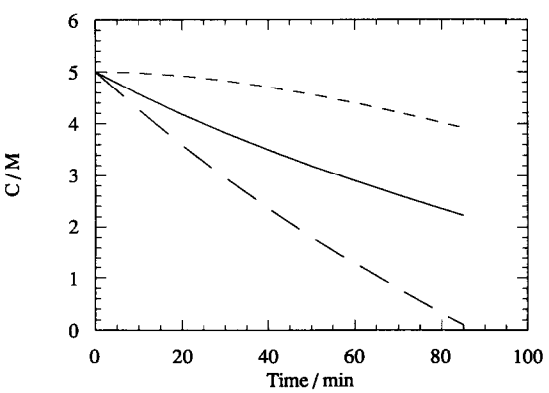

Fig. 2. Electrolyte concentration predicted for discharge of a lead/acid cell with 33.6 mA cm^{-2}; battery data from Sunu [6].

where a and b are constants; i is the current density (current per active surface area (I/S)). During the discharge, the active surface area of the electrodes is blocked by isolating lead sulfate; this leads to a continued decrease in available active surface area during the discharge. The Tafel equation can then be written as:

$$\eta = a + b \log I - b \log S \tag{7}$$

For discharge with constant current, the surface area decreases linearly, which gives the following equation for the overvoltage:

$$\eta = a + b \log\left(\frac{I}{S_0(1-q)}\right) \tag{8}$$

If the discharge current varies, the active surface area decreases in a more complicated way. At higher currents, the produced lead sulfate crystals are smaller and this results in a faster blocking of the active surface area. The introduction of a differential Peukert relation [5] is a method that has been used to take this effect into account. In the model presented here, an integrated Peukert equation is used for the change in active surface area during discharges, i.e.:

$$S = S_0\left(1 - \frac{1}{K_0}\int_0^t I^n \, dt\right) \tag{9}$$

Figure 3 shows how the cell voltage changes with time for a discharge with constant current, where the current and geometry of the cell are chosen so that blocking of active electrode surface by lead sulfate limits the discharge capacity.

During discharge, the zone where the electrochemical reaction takes place moves from the outer surface towards the centre of the electrode [2]. Therefore, the length of the current path in the electrolyte-filled pores increases with depth-of-discharge. In the model, this current transport in the pores results in an additional resistance. Due to the fact that the conductivity of the electrolyte is much lower than that of the solid electrode material (which in the model is neglected), this additional resistance increases with depth-of-discharge.

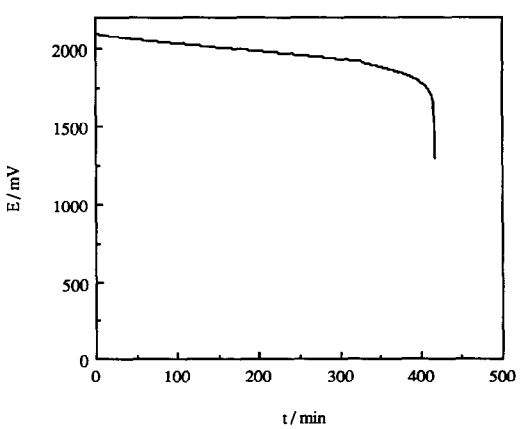

Fig. 3. Calculated cell voltage for a lead/acid battery discharged with a low current ($i = 8.4$ mA cm^{-2}) where surface blocking limits the discharge capacity; battery data from Sunu [6].

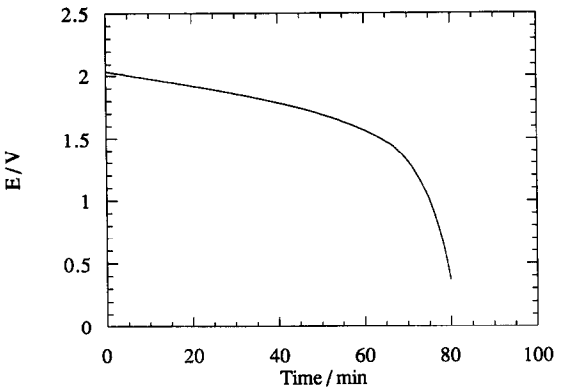

Fig. 4. Calculated cell voltage for a lead/acid battery discharged with a high current (i = 33.6 mA cm^{-2}) where acid depletion limits the discharge capacity; battery data from Sunu [6].

The resistance is determined by the effective conductivity of the pore electrolyte and the distance between the surface of the electrode and the reaction zone. In the model, the distance between the electrode surface and the reaction zone is assumed to be proportional to the depth-of-discharge. This gives the final expression for the overvoltage of the electrodes as:

$$\eta = a + b \log\left(\frac{I}{S_0}\right) - b \log\left(\frac{S}{S_0}\right) + I \frac{q}{q_0} \frac{1}{\kappa_{\text{eff}}} \tag{10}$$

Figure 4 shows a discharge curve according to eqn. (10) for a discharge current where acid depletion limits the discharge capacity, which manifests itself in a fast increase in the last term in eqn. (10).

The battery voltage is the sum of the cell voltages minus the ohmic drop in the interconnections and battery poles:

$$E_{\text{bat}} = NE_{\text{cell}} - IR_{\text{ext}} \tag{11}$$

Determination of the parameters in the model

The parameters necessary for simulating the lead/acid battery can be determined from data given in the literature. The concentration dependence of the equilibrium potential was calculated with following empirical relations [16] for the lead dioxide electrode:

$$E_{0,\,\text{PbO}_2} = 1628.2 + 73.92 \log m + 33.12 \log^2 m + 43.2 \log^3 m + 21.56 \log^4 m \tag{12}$$

and for the lead electrode:

$$E_{0,\,\text{Pb}} = -344.6 - 7.59 \log m - 30.53 \log^2 m - 30.5 \log^3 m - 12.05 \log^4 m \tag{13}$$

where m is the concentration in molality. A polynomial expression based on data for sulfuric acid at 25 °C [16] was used for the relationship between the molality and molarity:

$$m = 1.003c + 3.55 \times 10^{-2} c^2 + 2.17 \times 10^{-3} c^3 + 2.06 \times 10^{-4} c^4 \tag{14}$$

The electrolyte conductivity was calculated according to a equation proposed by Tiedemann and Newman [17]:

$$\kappa = \frac{c}{10} \exp\left(1.1104 + 0.199475c - 0.0160977881c^2 + \frac{3916.95 - 99.406c - \frac{72860}{T}}{T}\right) \quad (15)$$

The effective conductivity of the electrolyte in the porous electrodes, which is less than the free conductivity of the electrolyte, decreases during the discharge due to plugging of the pores by lead sulfate and due to decreasing sulfuric acid concentration. The free conductivity in 5 M sulfuric acid at 25 °C is 78 Ω^{-1} m^{-1} [16], whereas the effective conductivity for a fully recharged lead dioxide electrode is 7 Ω^{-1} m^{-1} [2] and 22 Ω^{-1} m^{-1} [4] for planer and tubular electrodes, respectively. The decrease in effective conductivity with decreasing electrode porosity was calculated using the Bruggman equation. The exponent in the Bruggman equation has been experimentally determined for the lead electrode as 1.5 [18]. The same value was used in the model for the positive electrode. The equation for the effective conductivity of the electrolyte in the electrodes can then be written as:

$$\kappa_{\text{eff}} = \kappa(c) \frac{\kappa^0_{\text{eff},0}}{\kappa^0} \left(\frac{\epsilon}{\epsilon_0}\right)^{1.5} \quad (16)$$

where the subscript 0 refers to the porosity of a fully charged electrode and the superscript 0 refers to the concentration in a fully charged cell.

The mean porosity of the electrodes changes with the degree of discharge due to the difference in molar volumes between the products and reactants:

$$\epsilon = \epsilon_0 - k(1 - \epsilon_0) \frac{q}{q_0} \quad (17)$$

where $k = (V_d - V_c)/V_c$. For the negative electrode $k = 0.971$, and for the positive electrode $k = 1.67$. The theoretical maximal discharge capacity per geometric area, q_0, was calculated from the amount of lead and lead dioxide in their respective electrodes and their molar volumes. This gave the following values for the electrodes in the lead/acid battery:

$$q_0 = 3.78 \times 10^9 (1 - \epsilon) d_p \text{ (positive electrode)} \quad (18)$$

$$q_0 = 2.11 \times 10^9 (1 - \epsilon) d_n \text{ (negative electrode)} \quad (19)$$

For the temperature and concentration dependence of the diffusion coefficient, Tiedemann and Newman [17] have proposed the following relation:

$$D = (1.75 + 0.260c) 10^{-9} \exp\left(7.29 - \frac{2174}{T}\right) \quad (20)$$

If the porous structure is assumed to exhibit the same hindrance to diffusion as the conductivity, the following expression can be used for the effective diffusion:

$$D_{\text{eff}} = D(c) \frac{\kappa^0_{\text{eff},0}}{\kappa^0} \left(\frac{\epsilon}{\epsilon_0}\right)^{1.5} \quad (21)$$

In this model, the electrode kinetics are described with Tafel equations, eqn. (6). The constant a and b have been determined from experimental polarization curves for porous battery electrodes. Polarization curves for tubular lead dioxide electrodes

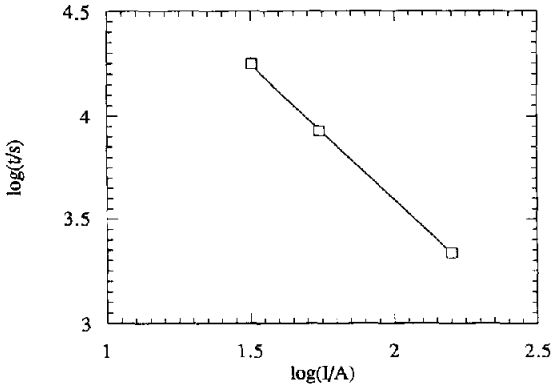

Fig. 5. Discharge time as a function of current for a 6-V lead/acid battery from Sonnenschein (Büdingen, Germany).

[19] give: $a = 30$ mV and $b = 30$ mV per decade. At low current densities, however, the Tafel equation is not valid, but can be replaced by the linear relation:

$$\eta = 0.91i \quad (i < \text{A m}^{-2}) \tag{22}$$

Polarization curves for the negative electrode exhibit two regions with different Tafel slopes. The constants for the two regions were determined from experimental data [3, 20]; the values were:

$a = -120$ mV, $b = 60$ mV per decade $\quad (i > 400$ A m$^{-2})$

$a = -13$ mV, $b = 18$ mV per decade $\quad (400$ A m$^{-2} > i > 50$ A m$^{-2})$

For low current densities, a linear relation was used, namely:

$$\eta = 1.16i \quad (i < 50 \text{ A m}^{-2})$$

The constants n and k_0 in the integral Peukert relation, eqn. (9), can be determined from discharge curves with constant current. From experimental data for a Sonnenschein (Büdingen, Germany), 6-V lead/acid battery discharged at rates $C1$, $C/3$ and $C/5$, the constants were calculated as $n = 1.3$ and $k_0 = 1.62 \times 10^6$, see Fig. 5. Since the influence from the separate electrodes could not be evaluated, the same values for the constants were used for both the positive and the negative electrodes.

The resistance of the intercell connections and terminal posts was determined by fitting calculated the internal resistance of the battery to experimental data, with R_{ext} as fitting parameter. The best agreement was achieved with $R_{ext} = 0.5$ mΩ, see Fig. 6.

Since the real geometry of the battery was unknown, some typical data for electrode thickness, distance between the electrodes, and total electrode area were used in the model, i.e.: $d_p = 2 \times 10^{-3}$ m; $d_n = 2 \times 10^{-3}$ m; $d_e = 2 \times 10^{-3}$ m; $A = 0.3$ m^2/cell.

The acid concentration in a fully recharged battery was assumed to be 5.1 M in all parts of the battery.

Results and discussion

The model has been tested against experimental discharge curves for a 6-V lead/acid battery from Sonnenschein. For discharge with constant current, a very good

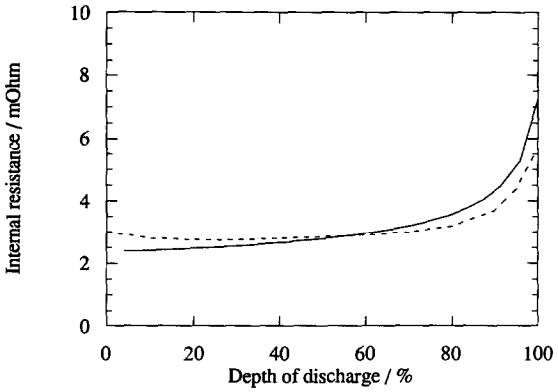

Fig. 6. Change in internal resistance during discharge; (----) experimental; (——) calculated.

agreement between experimental and calculated discharge curves was obtained. Figure 7 shows the discharge curves for three different currents. The divergence between the calculated and experimental voltages was less than 1% over the entire discharge range for all three currents.

The applicability of the model for simulating dynamic discharge has also been tested. Figure 8 presents a comparison of experimental and calculated discharge curves according to the RWE (Rhein. Westf. Elektrizitätswerke, Essen, Germany) electrical-vehicle test cycle (see Fig. 9). The calculated voltage at the two different currents used in this cycle is in good agreement with the experimental results. At the rest periods of the cycle, the model predicts an excessively high voltage. This may be explained by the slow recovery of the voltage of the positive active mass. The voltage at the rest periods is, however, of less importance for the simulation of an electrical vehicle, since it does not influence the calculated power output from the battery. The battery capacity predicted by the model for discharge according to the RWE cycle was ~7% too low.

The influence of the different parameters on the calculated voltage and capacity has not been evaluated. It would probably be possible to further simplify the model by neglecting those parameters that exert only a small influence on battery performance. The model can also be improved by fitting the parameters. This is, however, beyond the scope of the present work, the purpose of which was to evaluate whether it is possible to simulate the behaviour of the lead/acid battery with a model using integral mean values instead of the time-consuming calculation of gradients in the porous electrodes. Fitting different parameters to obtain a better agreement between calculated and experimental discharge curves for a special battery was not the purpose of this model, which was rather to simulate a lead/acid battery with a simple model based on mainly literature data.

Conclusions

A simplified model, which neglects concentration, potential and current gradients in the porous electrodes, can be used to simulate the discharge performance of the lead/acid battery. The following observations have been made:

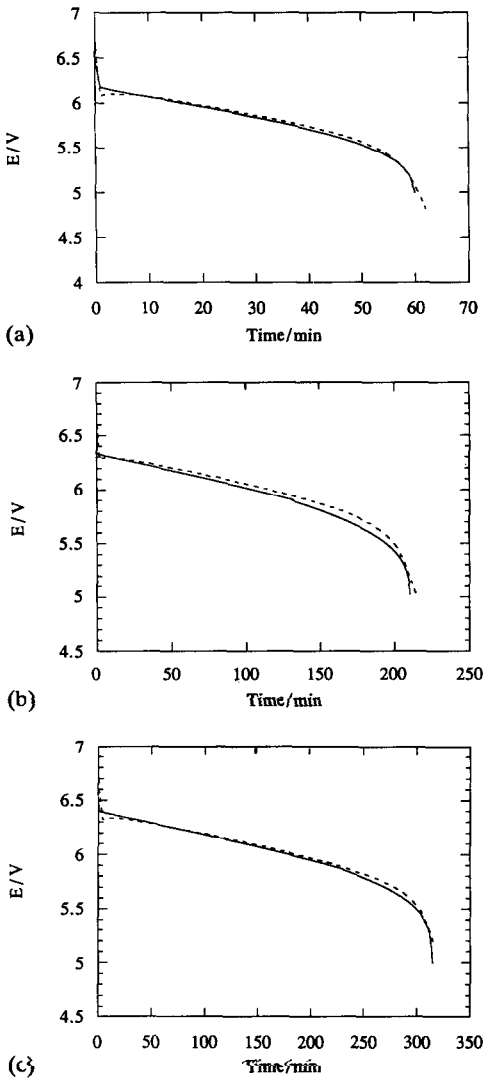

Fig. 7. Comparison of (——) calculated and (– – –) experimental galvanostatic discharge curves: (a) $I = \mathcal{E}/2$; (b) $I = \mathcal{E}/3$; (c) $I = \mathcal{E}/5$.

(i) The model can predict limitations of the discharge capacity by different phenomena, such as electrolyte depletion in the pores and coverage of the electroactive surface by the precipitated reaction product, as determined by the cell geometry and discharge mode.

(ii) The model can be used for the simulation of dynamic processes, where high-current pulses cause both lasting effects (e.g., surface blocking by lead sulfate) and effects from which the battery recovers in rest periods (e.g., acid depletion).

(iii) The model can simulate the lead/acid battery with reasonable accuracy, without experimental determination of different parameters, and using literature data only.

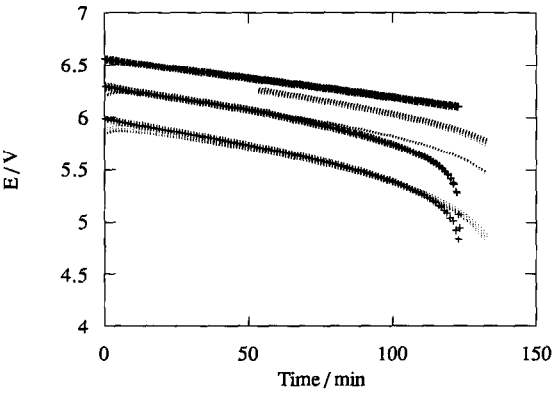

Fig. 8. Comparison of (+ + +) and (· · · · ·) experimental discharge curves for battery discharged according to the RWE cycle (Rhein. Westf. Elektrizitätswerke, Essen, Germany).

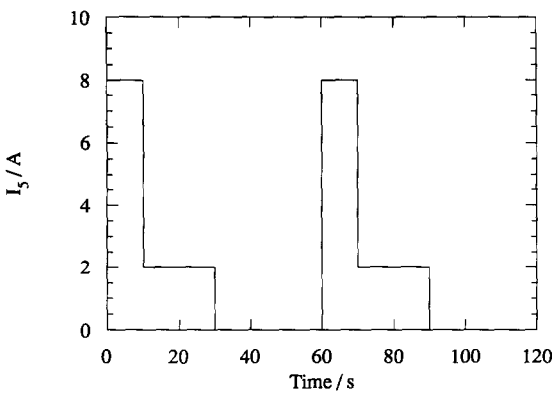

Fig. 9. Current profile for the RWE-cycle for lead/acid batteries (Rhein. Westf. Elektrizitätswerke, Essen, Germany).

Acknowledgements

The study was financially supported by AB Volvo and the Swedish National Board for Industrial and Technical Development.

Mr Romare, AB Volvo, and Cartell Generic are also grateful acknowledged for providing the experimental data.

List of symbols

A	electrode area, m^2
a	Tafel constant, V
b	Tafel slope, V per decade
c	concentration, mol l^{-1}
D	diffusion coefficient, m s^{-1}
d	thickness, m

E	voltage, V
F	Faraday constant, 96487 C mol^{-1}
I	current, A
i	current density, A m^{-2}
i_0	exchange current density, A m^{-2}
K	Peukert constant
n	Peukert exponent
m	concentration, mol kg^{-1}
N	number of cells
R	resistance, Ω
q	charge output, A m^{-2}
S	active surface area, m^2
T	temperature, K
t	time, s
t_+	transfer number of cations
V	molar volume, m^3 mol^{-1}

Greek letters

ϵ	porosity
κ	conductivity, Ω^{-1} m^{-1}
η	overvoltage, V

Subscripts

bat	battery
cell	cell
c	charged state, Pb or PbO_2
d	discharged state, $PbSO_4$
e	electrolyte between the electrodes
eff	effective accounting to porous medium
ext	external
n	negative electrode
p	positive electrode
0	fully charged battery

References

1 T.V. Nguyen, R.E. White and H. Gu, *J. Electrochem. Soc., 137* (1990) 2953.
2 D. Simonsson, *J. Appl. Electrochem., 3* (1973) 261.
3 P. Ekdunge and D. Simonsson, *J. Appl. Electrochem., 19* (1989) 136.
4 J. Landfors and D. Simonsson, *J. Electrochem. Soc., 139* (1992) 2768.
5 K. Micka and I. Rousar, *Electrochim. Acta, 21* (1976) 599.
6 G. Sunu, in R. White (ed.), *Electrochemical Cell Design,* New York, 1983, p. 357.
7 H. Gu, T.V. Nguyen and R.E. White, *J. Electrochem. Soc., 134* (1987) 2953.
8 E.C. Dimpault-Darcy, T.V. Nguyen and R.E. White, *J. Electrochem. Soc., 135* (1986) 278.
9 W. Peukert, *Elektrotech. Z., 18* (1897) 287.
10 R. Kaushik and I.G. Mawston, *J. Power Sources, 28* (1989) 161.
11 C.M. Shepherd, *J. Electrochem. Soc., 112* (1965) 657.
12 E. Hyman, W.C. Spindler and J.F. Fatula, *AIChE Symp. Ser. 83, 254* (1987) 78.
13 D. Gidaspow and B.S. Baker, *J. Electrochem. Soc., 120* (1973) 1005.

14 U. Teutsch, F. Böttcher and A. Winsel, *Ber. Bunsenges. Phys. Chem., 92* (1988) 1297.
15 J. Newman and W. Tiedemann, *Am. Inst. Chem. Eng. J., 21* (1975) 25.
16 H. Bode, *Lead-Acid Batteries,* Wiley, New York, 1977.
17 W.H. Tiedemann and J. Newman, in S. Gross (ed.), *Battery Design and Optimisation,* Proc. Vol. 79-1, The Electrochemical Society, Princeton, NJ, USA, 1979, p. 23.
18 P. Ekdunge and D. Simonsson, *J. Appl. Electrochem., 19* (1989) 127.
19 J. Landfors and D. Simonsson, *J. Electrochem. Soc., 139* (1992) 2760.
20 P. Ekdunge, M. Lindgren and D. Simonsson, *J. Electrochem. Soc., 135* (1988) 1613.